An Operational Resilience Metric for Modern Power Distribution Systems

Tyler Phillips
National & Homeland Security
Idaho National Laboratory
Idaho Falls, Idaho, USA
tylerphillips1@u.boisestate.edu

Timothy McJunkin
Power & Energy Systems
Idaho National Laboratory
Idaho Falls, Idaho, USA
timothy.mcjunkin@inl.gov

Craig Rieger
National & Homeland Security
Idaho National Laboratory
Idaho Falls, Idaho, USA
craig.rieger@inl.gov

John Gardner
Mechanical & Biomedical Engineering
Boise State University
Boise, Idaho, USA
jgardner@boisestate.edu

Hoda Mehrpouyan
Computer Science
Boise State University
Boise, Idaho, USA
hodamehrpouyan@boisestate.edu

***Abstract*—The electrical power system is the backbone of our nations critical infrastructure. It has been designed to withstand single component failures based on a set of reliability metrics which have proven acceptable during normal operating conditions. However, in recent years there has been an increasing frequency of extreme weather events. Many have resulted in widespread long-term power outages, proving reliability metrics do not provide adequate energy security.**

As a result, researchers have focused their efforts resilience metrics to ensure efficient operation of power systems during extreme events. A resilient system has the ability to resist, adapt, and recover from disruptions. Therefore, resilience has demonstrated itself as a promising concept for currently faced challenges in power distribution systems.

In this work, we propose an operational resilience metric for modern power distribution systems. The metric is based on the aggregation of system assets adaptive capacity in real and reactive power. This metric gives information to the magnitude and duration of a disturbance the system can withstand. We demonstrate resilience metric in a case study under normal operation and during a power contingency on a microgrid. In the future, this information can be used by operators to make more informed decisions based on system resilience in an effort to prevent power outages.

***Index Terms*—Resilience, Adaptive Capacity, Power distribution**

I. Introduction

Today's modern society has become increasingly dependent on the safety and efficiency of modern control systems. At the foundation of our social and economic way of life, you will find the electrical power system. It constitutes the most vital component of the nation's interdependent critical infrastructure systems. To ensure a constant supply of electrical power, utilities and researchers have designed and operated the power system under the consideration of a set of reliability metrics. These metrics account for normal weather conditions and component failure but do not consider extreme events [1] as it is generally not cost effective [2].

In the early stages of power system construction, relatively little attention was given to the distribution networks when compared with generation and transmission. Generation and transmission outages are large impact events, whereas distribution outages have smaller localized effects. However, analysis of practical utility failure registers and fault statistics reveals that distribution networks contribute the most to customer interruptions and failure events [3]. The data shows that 90% of the power outages occur in the distribution system alone [4].

Complete disaster-resistant protection of the distribution system is highly impractical, requiring far too much investment [5]. Therefore, researchers have begun to focus their efforts on resilience, not reliability, metrics. The concept of reliability and resilience are similar but have distinct differences in both scale and duration. Reliability research concentrates on small-scale random faults of power system components caused by internal factors [6]. For example, reliability encompass the N-1 contingency planning or a single component failure. At the basic level, it ensures that no single point of failure would cause the entire system to stop working. In contrast, resilience considers extreme conditions, or N-k failures, where k may extend well beyond a single failure point. Resilience anticipates that during extreme events a certain amount of degradation to the system is unavoidable. Thus, it can be said that resilience is characterized by a systems ability to resist, respond, and recover from a disturbance or attack in order to maintain core operations [7].

Electrical component failures during extreme weather events such as hurricanes, winter storms, flooding, wildfires, etc., push well beyond the limitations of the current distribution system which has been design to meet reliability metrics. In the United States, between 2003 and 2012, extreme weather events caused an estimated 679 widespread power outages, affecting at least 50,000 customers [4]. Notable events include

This paper was supported by the U.S. Department of Energy's Office of Energy Efficiency and Renewable Energy under the Solar Energy Technology Office Award Number DE-0008775.

978-1-7281-8915-4/20/$31.00 ©2020 IEEE
DOI 10.1109/QRS-C51114.2020.00065

Hurricane Katrina [8], Hurricane Sandy [9], and the wildfires across California [10] which forced the utility company to de-energize power lines in an effort to mitigate the risk of starting new fires, resulting in widespread blackouts. Making matters worse, our energy infrastructure is aging [11] and climate change is expected to continually increase the frequency and intensity of extreme weather [4]. A 2012 study [12] estimates the cost of weather-related outages to the tune of $25 to $70 billion annually. Moreover, these prolonged power outages can put the public at a significant risk, having the potential for loss of life. Data indicates that the 2003 blackout in New York resulted in approximately 90 deaths [13]. In light of these factors, it is of upmost importance for researchers to address the growing concern of electrical power supply during extreme weather events. New methodologies which enable utilities to effectively manage power systems must be developed.

In this work, we present a novel real-time operational resilience metric that utilizes the controllable assets in modern distribution systems. The metric is an operational aggregation of assets adaptive capacity in real and reactive power. It indicates the magnitude and duration of a disturbance a system is capable of withstanding, and maintain load demand and stability in voltage and frequency.

The rest of this paper is organized as follows: Section II gives an introduction to resilience and a literature review. The modern distribution system (MDS) and background on power stability is discussed in sectionIII. We introduce our resilience metric and give the mathematical details in Section IV. Finally, the conclusion and future work are covered in Section VI.

II. Resilience in Power Systems

Pioneering work in resilience of engineering systems is presented by Hollnagel, Woods, and Leveson in [14]. Many definitions have been coined by well respected organizations in engineering literature [15]–[19], policy directives [20], and the academic community [21]. A general commonality among sources are the ability to anticipate a possible disaster, adopt effective measures to decrease loss of load and system component failure before and during the disaster, and restore power quickly through controlled reconfiguration. Quantification of resilience in power systems is an emerging field. It is an important open area of research, of great interest to utilities and stakeholders.

To date, power systems are regulated based upon reliability metrics. This dates back to the Energy Policy Act of 2005 [22], where Congress gave the Federal Energy Regulatory Commission authority to oversee the reliability of the bulk-power systems. The purpose was to ensure the reliable operation where an instability, uncontrolled separation, or cascading failures would not occur as a result of a sudden disturbance. There are two main metrics used to measure the reliability; the system average interruption duration index and the system average interruption frequency index. However, some jurisdictions consider storm related outages as extreme events, and thus, do not include them as inputs into the reliability metrics [23].

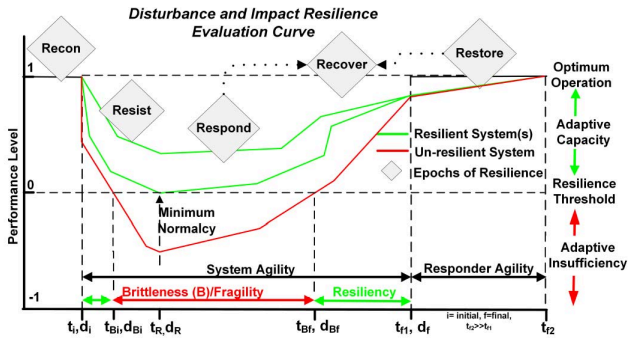

Fig. 1. The disturbance and impact resilience evaluation curve, showing the 5R's of resilience. Image adapted from [30].

There have been several proposed resilience metrics, such as the resilience triangle and trapezoid. The resilience trapezoid is an extension of the resilience triangle proposed in [24] by Tierney and Bruneau. Unlike the triangle which only considers the disturbance of a system, the trapezoid assesses the resilience through three phases; the disturbance, degradation, and the restorative state. The resilience trapezoid has been applied to a power system framework as proposed by Panteli et. al [25], which extends the works in [26]–[29].

Another proposed resilience approach is introduced by Rieger [30]. In this work he takes a controls systems perspective but doesn't apply the metric directly to power systems. System resilience is shown by the notional disturbance and impact resilience evaluation (DIRE) curve in Fig. 1. The novel concept introduced is the idea of a resilience threshold, or the maximum acceptable level of degradation to the system. This degradation level may be defined by a percentage of loss load in the system, ability to retain critical loads, etc. The performance level from optimal operation to the resilience threshold is defined by the systems adaptive capacity. The adaptive capacity can be defined as the ability of the system to adapt or transform from an impact event. An adaptive insufficiency can be considered the inability of the system to adapt or transform from an impact, indicating an unacceptable performance loss due to the given disturbance.

In [31], Woods describes an aspect of assessing a systems resilience is whether the system is known to be near an operation boundary condition. This provides information about how well the system can stretch in response to a future disturbance. In the context of power systems, McJunkin and Rieger expand this concept and introduce a resilience metric to evaluate the design of modern distribution systems (MDS) [32]. Their approach is based on the adaptive capacity of a system, defined by an asset or aggregation of assets. In this work, they demonstrate the temporal adaptive capacity, or amount of flexibility or stretch, in the real and reactive power of the controllable assets while also considering energy limitations. The resulting metric can by represented by a three dimensional surface, referred to as a manifold, that represents the maximum adaptive capacity in real and reactive power

over time. The metric can be thought of as a mapping to the DIRE curve, indicating the maximum disturbance in amplitude and duration due to cyber or physical disturbances that can be withstood.

The most recent contributions of the resilience metric proposed in [32] have been developed as a design tool for MDS. The metric uses a neutral bias assumption to describe the adaptive capacity of the assets which limits the ability to accurately model many assets. In addition, the metric does not lend itself well for use as a real-time operational metric. Therefore, the goal of this paper is to develop the metric to have a more accurate representation of the asset adaptive capacity. In addition, we will bring the metric to a state where it is suitable to be used as a real-time operational tool. Therefore, it and can be utilized by control operators to make resilience based decisions before, during, and after disturbances. The details of the extension of the metric are covered in section IV. First, a background on MDS is covered in the following section.

III. Power Distribution System

In this section, a brief introduction to the modernization of the power grid is given. Then the concepts of power stability in voltage and frequency necessary for the development of the metric proposed in this paper are covered in sufficient detail.

A. Grid Modernization

The current modernization of the electrical power system, has presented a dramatic shift in the way power is generated and transmitted. It is moving from the traditional centralized generation to a more distributed power generation architecture. The MDS integrates information and operational technologies which can monitor, communicate, and control assets in real-time. It is predicted that these systems will include a high penetration of controllable distributed assets in generation and storage, as well as controllable loads. Control of these assets have many purposes, including support of the voltage and frequency across the distribution network, economic benefits, and reliable utilization of interconnections such as power lines, transformers, and switches.

This evolving landscape has added a new layer of complexity to distribution systems. It presents many new technical challenges and opportunities for researchers. For example, what metric best describes the systems resilience and how should these metrics be utilized to make control decisions during normal operation or before, during, and after extreme events? The modernization of the grid has a tremendous potential for increasing resilience but much work is still needed in how to accomplish it. In this context, researchers have suggested numerous resilience based improvements in areas including microgrids [33], [34], circuit reconfiguration [35]–[42], improved dispatch and scheduling of resources [43]–[45], and flexible local resources, such as generation, load, and energy storage [46].

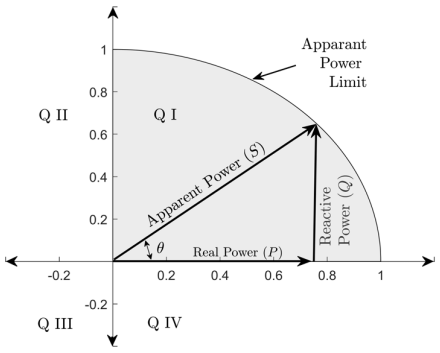

Fig. 2. Normalized apparent power, S, in quadrant I of the complex S-plane. The highlighted region represents the domain or reachable output in real and reactive power.

B. Power and Stability

Stability of the distribution system is defined in terms of voltage and frequency. Frequency stability requires balancing of the generation of real power, P, and the load demand. On the other hand, voltage stability requires the balancing of reactive power, Q, across the network due to different types of loading on the system. Therefore, a resilience metric must address both the real and reactive power to be extensible in distribution systems. The real and reactive power components define a systems apparent power, S in the complex S-plane where

$$S(\theta) = \sqrt{P^2 + Q^2} \tag{1}$$

where the real power in relation to the apparent power is

$$P(\theta) = S\cos(\theta) \tag{2}$$

and the reactive power is

$$Q(\theta) = S\sin(\theta) \tag{3}$$

here θ is the angle measured from horizontal. In power systems this angle is often referred to as the power factor angle, given as

$$\theta = \arctan\left(\frac{Q}{P}\right) \tag{4}$$

In this paper, the angle θ is the measurement from 0 to 2π. Here, the left hand plane, $\pi/2 < \theta < 3\pi/4$, is where an asset acts as a sink absorbing power from the system.

The normalized maximum apparent power at power factor angle θ is depicted in the S-plane in Fig. 2. Here, only quadrant I is shown, where real and reactive power are positive. The highlighted region is the domain or reachable output in real and reactive power. In the following section we use this principals to define the domain of assets power output used in our operational adaptive capacity metric.

IV. Adaptive Capacity Methodology

This section describes the mathematical background to calculate the operational adaptive capacity resilience metric herein proposed. The metric is based on the adaptive capacity

of the assets, which is a measure of their control ability to move from the current operating point in both real and reactive power over time. Assets must be described by a set of operational characteristics which include the nameplate rated capacity, energy capacity, latency, and rate of change limitations. Using these characteristics, the general process to calculate the adaptive capacity is as follows: determine the control domain of the real and reactive power, determine the flexibility from the current operating point, then account for latency and ramp rates, then impose energy constraints.

A. Real and Reactive Power Domain

The real and reactive power domain, or capability of the asset, is denoted $P_{\in}$ and $Q_{\in}$, respectively. The assets nameplate capacity defines the real power maximum, $P_{\max}$, and minimum, $P_{\min}$, as well as the reactive power maximum, $Q_{\max}$, and minimum, $Q_{\min}$. Thus, the first limit placed on the domain of the real power is

$$P_{\min} \leq P \leq P_{\max} \tag{5}$$

and the reactive power is

$$Q_{\min} \leq Q \leq Q_{\max} \tag{6}$$

here, the maximum is assumed to be in the positive plane and the minimum in the negative plane, given mathematically for the real power

$$P_{\min} \leq 0 \leq P_{\max} \tag{7}$$

and for the reactive power

$$Q_{\min} \leq 0 \leq Q_{\max} \tag{8}$$

These values are then used to determine the bounding constraints of the asset in the complex S-plane, given as

$$S(\theta) \leq \left(P^2 + Q^2\right)^{\frac{1}{2}} \tag{9}$$

here, the real and reactive power is a function of the power factor angle and dependant on the maximum power in each quadrant of the S-plane. The calculation for the apparent power constraint for quadrant I to quadrant IV is then given respectively as

$$\underset{0\leq\theta\leq\frac{\pi}{2}}{S(\theta)} \leq \left(P_{\max}^2 \cos(\theta) + Q_{\max}^2 \sin(\theta)\right)^{\frac{1}{2}} \tag{10}$$

$$\underset{\frac{\pi}{2}\leq\theta\leq\pi}{S(\theta)} \leq \left(P_{\min}^2 \cos(\theta) + Q_{\max}^2 \sin(\theta)\right)^{\frac{1}{2}} \tag{11}$$

$$\underset{\pi\leq\theta\leq\frac{3\pi}{2}}{S(\theta)} \leq \left(P_{\min}^2 \cos(\theta) + Q_{\min}^2 \sin(\theta)\right)^{\frac{1}{2}} \tag{12}$$

$$\underset{\frac{3\pi}{2}\leq\theta\leq 2\pi}{S(\theta)} \leq \left(P_{\max}^2 \cos(\theta) + Q_{\min}^2 \sin(\theta)\right)^{\frac{1}{2}} \tag{13}$$

Using the rated power and limits in the S-plane, the asset capability in the real and reactive power can be calculated. In the positive plane the minimum of the two constraints will define the boundary of the domain. In the negative plane, the absolute minimum of the two constraints defines the domain boundary. Therefore, the real power domain for quadrants I and IV, where the real power is positive, is given by

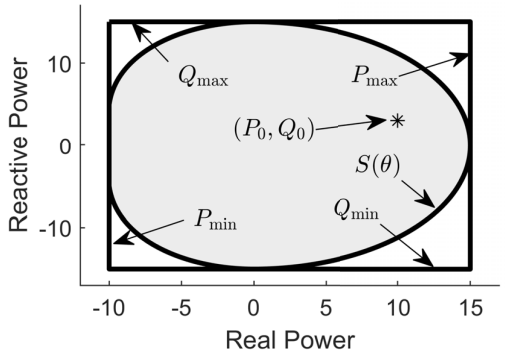

Fig. 3. The shaded region represents an assets real and reactive power domain based on its rated nameplate power capacity. The negative real power represents an asset absorbing power from the grid, such as battery storage when charging.

$$\underset{\frac{3\pi}{2}\leq\theta\leq\frac{\pi}{2}}{P(\theta)} \leq \min\left[S\cos(\theta),\ P_{\max}\right] \tag{14}$$

and the domain for quadrants II and III, where the real power is negative is

$$\underset{\frac{\pi}{2}\leq\theta\leq\frac{3\pi}{2}}{P(\theta)} \geq -\min\left[|S\cos(\theta)|,\ |P_{\min}|\right] \tag{15}$$

Similarly, the domain of reactive power in quadrants I and II is given by

$$\underset{0\leq\theta\leq\pi}{Q(\theta)} \leq \min\left[S\sin(\theta),\ Q_{\max}\right] \tag{16}$$

and in quadrants III and IV are

$$\underset{\pi\leq\theta\leq 2\pi}{Q(\theta)} \geq -\min\left[|S\sin(\theta)|,\ |Q_{\min}|\right] \tag{17}$$

Using the real and reactive power domain in the positive and negative quadrants, the union of the two gives the overall domain. For the real power this is given as

$$P_{\in}(\theta) = \left\{P\middle|\frac{3\pi}{2} \leq \theta \leq \frac{\pi}{2}\right\} \cup \left\{P\middle|\frac{\pi}{2} \leq \theta \leq \frac{3\pi}{2}\right\} \tag{18}$$

and similar for the reactive power

$$Q_{\in}(\theta) = \left\{Q\middle|0 \leq \theta \leq \pi\right\} \cup \left\{Q\middle|\pi \leq \theta \leq 2\pi\right\} \tag{19}$$

The domain of the asset real and reactive power capability is depicted by the shaded region in Fig. 3. It should be noted that some assets, such as solar, wind, and hydro, should not be considered to have constant rated limits and the domain may need to be updated. For example, solar generation is dependant on the real-time solar irradiation and therefore should be updated as solar conditions change. Next, we will discuss how the power flexibility is calculated using the operational power output.

B. Real and Reactive Flexibility

The amount of flexibility the asset has in the real and reactive power from the operating point is denoted as, P_Δ and Q_Δ, respectively. This flexibility is calculated using the real and reactive power domain of the asset and the current operation point of the asset, P_0 and Q_0. Thus, it is a transformation of the power domain around the operating point, given as

$$P_\Delta(\theta) = P_\in - P_0 \tag{20}$$

and the flexibility of the reactive power is the same transformation using the reactive power domain and the current operating point

$$Q_\Delta(\theta) = Q_\in - Q_0 \tag{21}$$

Here, and in further adaptive capacity derivation, θ is the angle measured from the operating point. The resulting flexibility is depicted in the top plot of Fig. 4. However, the temporal characteristics of the asset, shown in the bottom plot of Fig. 4, need to be accounted for and are developed in the following section.

C. Latency and Ramp Rate

The latency of an asset is the time delay before changes to the power output can be made. It may consist of multiple factors including starting latency or a control latency. Starting latency is a property of the asset, for example, a diesel generator can't supply power right when turned on. Control latency is the time required between data being received, adjustments made to the output power, computationally or by an operator, to the time the control command is received by the asset. For the purpose of this paper, we consider all latency's to be aggregated into a single latency variable, λ.

The ramp rate defines how quick an asset can ramp up or down, after the latency, from the current operating position over time, t. The real power output when ramping up is given as

$$P(t)^+ = \begin{cases} 0, & \text{if } t \le \lambda \\ \frac{dP^+}{dt}(t-\lambda) & \text{if } t > \lambda \end{cases} \tag{22}$$

and when ramping down is

$$P(t)^- = \begin{cases} 0, & \text{if } t \le \lambda \\ \frac{dP^-}{dt}(t-\lambda) & \text{if } t > \lambda \end{cases} \tag{23}$$

Similarly, the reactive power is given as

$$Q(t)^+ = \begin{cases} 0, & \text{if } t \le \lambda \\ \frac{dQ^+}{dt}(t-\lambda) & \text{if } t > \lambda \end{cases} \tag{24}$$

when ramping up, and

$$Q(t)^- = \begin{cases} 0, & \text{if } t \le \lambda \\ \frac{dQ^-}{dt}(t-\lambda) & \text{if } t > \lambda \end{cases} \tag{25}$$

when ramping down. The latency and ramp rate constraints are depicted by the temporal flexibility in real power shown in the bottom plot in Fig. 4. Here, the shaded region represents the real power domain and the bounds are defined by the latency and ramp rates from the operation point, the maximum flexibility, and energy constraints. The following section describes the energy constraint of the asset.

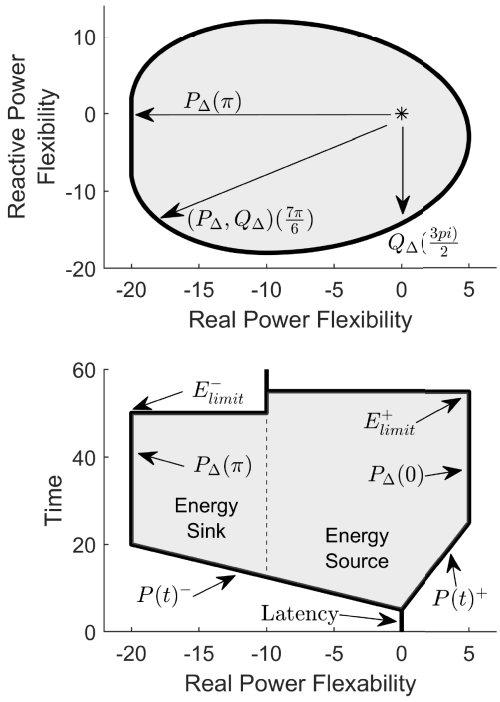

Fig. 4. Top plot shows an assets real and reactive power flexibility from its current operating point. The bottom plot shows the temporal flexibility from the operating point which considers latency, ramp rates, and energy limits.

D. Energy Constraints

It is possible that assets are constrained with energy limitations in the amount of real power when acting as a source providing power, or as a sink absorbing power. In the case of battery storage, it is constrained on both ends where it has an initial energy of E_0, and can only be charged (sink) to 100%, or $E_{\max}$, and it can only output power (source) until it is fully drained at 0%, or $E_{\min}$. The energy of the system changes as

$$E(t) = E_0 + \int_{t=0}^{t} P(t) * dt \tag{26}$$

where $P(t)$ is the operating real power over time. When an asset runs out of energy or the ability to absorb energy, the real power must go to zero. The necessary mathematical details have been covered to give the adaptive capacity equations covered in the next section.

E. Adaptive Capacity and Aggregation of Assets

The adaptive capacity of the asset is the bounded region between the flexibility and the temporal constraints in the positive and negative planes with respect to the operating point. The real power in the positive plane is given as

$$P_{\text{AC}}(\theta, t) = \min\left[P(t)^+,\ P_\Delta(\theta)\right] \tag{27}$$
$$\frac{3\pi}{2} \le \theta \le \frac{\pi}{2}$$

and the negative plane

$$P_{\underset{\frac{\pi}{2}\leq\theta\leq\frac{3\pi}{2}}{\text{AC}}}(\theta,t) = -\min\left[|P(t)^{-}|,\ |P_{\Delta}(\theta)|\right] \tag{28}$$

The reactive power it is given as

$$Q_{\underset{0\leq\theta\leq\pi}{\text{AC}}}(\theta,t) = \min\left[Q(t)^{+},\ Q_{\Delta}(\theta)\right] \tag{29}$$

in the positive plane, and

$$Q_{\underset{\pi\leq\theta\leq2\pi}{\text{AC}}}(\theta,t) = -\min\left[|Q(t)^{-}|,\ |Q_{\Delta}(\theta)|\right] \tag{30}$$

for the negative plane. The resulting adaptive capacity using the ongoing example in this section is depicted by the manifold in Fig. 5. The manifold surface represents the maximum change the asset can make in real and reactive power, from the current operating point, over time. Recall that the x/y axis represent the adaptive capacity from the operating power. Therefore, when the energy limit has been reached the output power goes to zero which is indicated by the dashed line separating where the asset transitions between a sink and a source.

It is expected that the MDS will comprise a collection of distributed assets. The adaptive capacity may be an aggregation of local assets, such as a microgrid. The aggregation of assets determines the adaptive capacity of the controllable assets in the microgrid including the network connection. The aggregation in terms of real power is

$$P_{\text{AC}}(\theta,t) = \sum_{k=1}^{n} P_{\text{AC}_k} \tag{31}$$

and the reactive power is given by

$$Q_{\text{AC}}(\theta,t) = \sum_{k=1}^{n} Q_{\text{AC}_k} \tag{32}$$

where n represents the total number of assets. The following section will demonstrate how this metric can be utilized as an operational metric.

F. Real-Time Operational Metric

Power distribution is a real-time system, therefore it's imperative that a resilience metric has the ability to reflect the real-time operation and conditions on the system. In this context, our algorithm updates the adaptive capacity using threshold triggers in power outputs, energy changes, and environmental conditions which we denote C. Relevant environmental conditions depend on the assets in the system but may include factors such as solar irradiation, wind velocity, head pressure, etc... The operational metric is outlined by Algorithm 1.

V. Case Study

In this section, we demonstrate the adaptive capacity resilience metric proposed using the modified Institute of Electrical and Electronics Engineers (IEEE) 33-bus distribution system. We first introduce the modified IEEE 33-bus system and use a selected portion, or microgrid, to demonstrate in

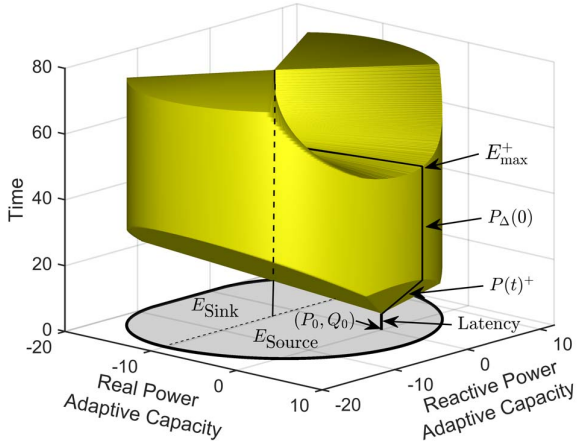

Fig. 5. Asset's adaptive capacity manifold which represents the maximum change in real and reactive power, from current operation, over time.

Algorithm 1: Real-Time Adaptive Capacity Algorithm

Input : System assets, Real-time system data
Output: Assets adaptive capacity

begin
  Initialize: $P_{\in}, Q_{\in}$
  while system running
    $P_{\delta} = |P_{0_{n-1}} - P_{0_n}|$
    $Q_{\delta} = |Q_{0_{n-1}} - Q_{0_n}|$
    $E_{\delta} = |E_{0_{n-1}} - E_{0_n}|$
    $C_{\delta} = |C_{0_{n-1}} - C_{0_n}|$
    if any $\delta >$ threshold
      Update $P_{\in}, Q_{\in}$
      Update P_{Δ}, Q_{Δ}
      for time = 0 to t_{end}
        Update $P(t), Q(t)$
        Update $E(t)$
        for $\theta = 0$ to 2π
          Solve $P_{\text{AC}}(\theta, t)$
          Solve $Q_{\text{AC}}(\theta, t)$
        end
      end
    end
    for k=1 to n
      $\sum P_{\text{AC}_k}(\theta, t)$
      $\sum Q_{\text{AC}_k}(\theta, t)$
    end
  end
end

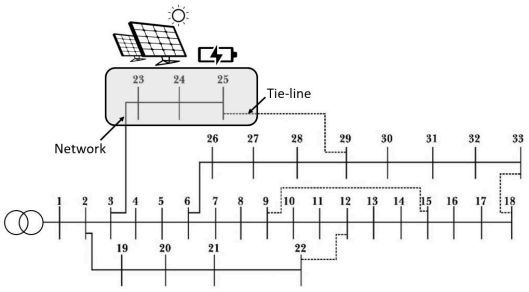

Fig. 6. IEEE 33-bus distribution system model. Image adapted from [47].

a case study the resilience of the system under two different scenarios. The first case represents the system under normal operation and the second represents a scenario where the network line experiences an outage.

A. IEEE 33-bus Model

The original IEEE model was designed as a radial network configuration. However, many studies have adapted the model to include tie-lines, thus, resembling a MDS meshed network, shown in Fig. 6. Here, the section used for this study has been highlighted and additional solar and battery storage assets have been added. The capacity limitations on the power line conductor for the network is given as $1,050$ kW and $1,050$ kVAR, and the tie-line limits are 500 kW and 500 kVAR for real and reactive power, respectively. Loading on buses 23-25 for the real power is 90, 420, and 420 kW, and the reactive power is 50, 200, and 200 kVAR, respectively.

To resemble a MDS solar generation and battery storage asset have been added to the model. Their limits are based on a high penetration of DERs. The maximum power is 30% of the maximum load which can be supplied by the network conductor, 315 kW. The battery storage is assumed to have a total capacity of 1,260 kWh, i.e. under its max output (315 kW) it would go from fully charged to empty in four hours. The asset operational characteristics are given in Table I.

B. Simulation and Results

Two scenarios are considered to demonstrate the difference in adaptive capacity of the system assets acting as a micro-grid. The first case is under what can be considered normal operation and the second case is when network connection has been lost, such as a storm outage or potentially a cyberattack, where the attacker forces a breaker open. For these cases, the loading conditions on the system are assumed to be constant and the assets operational power output for both cases is given in Table I.

Under normal operation the load is fully supplied by the network and the solar generation is therefore being used to charge the battery storage asset which is currently assumed to be at 75% of capacity. The adaptive capacity is calculated for each of the assets and their manifolds are shown in the top two rows of Fig. 7, and the aggregation of the assets is shown by the large manifold at the bottom. The temporal flexibility of

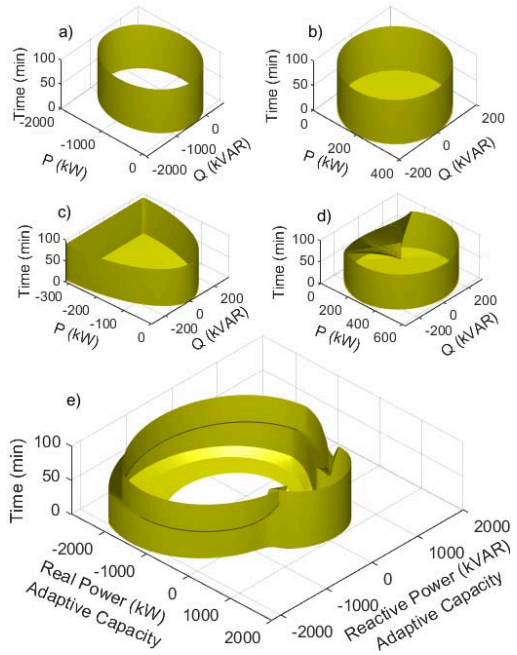

Fig. 7. Resulting adaptive capacity of the assets under normal conditions: a) network connection, b) tie-line connection, c) solar generation, d) battery storage, and e) aggregation of the assets.

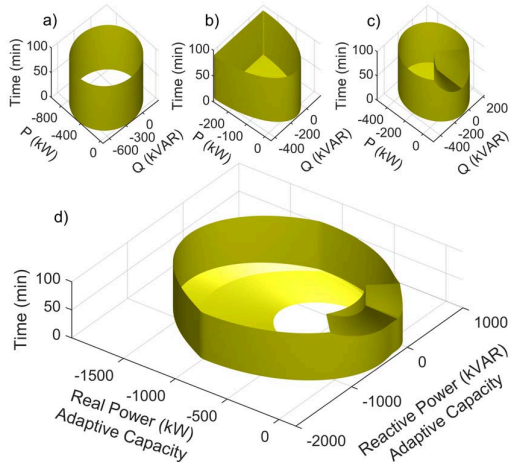

Fig. 8. Resulting adaptive capacity of the assets when network connection lost: a) tie-line connection, b) solar generation, c) battery storage, and d) aggregation of the assets.

the assets real and reactive power in the positive and negative direction is shown in the top of Fig. 9.

The second case which considered a loss of the network connection with reconfiguration where the tie-line is being used to supply power. However, based on its limiting characteristics, it cannot fully support the high loading conditions. In this situation, the solar asset is supplying power at its full capacity and the battery storage is able to supply the reaming load. In this case, we assume that the battery has 197 kWh of

TABLE I
ASSETS POWER PARAMETERS.

	Limits				Case I		Case II	
Asset	$P_{\max}$	$P_{\min}$	$Q_{\max}$	$Q_{\min}$	P_0	Q_0	P_0	Q_0
Network	1,050	-1,050	1,050	-1,050	930	450	0	0
Tie-line	500	-500	500	-500	0	0	450	217
Solar PV	315	0	315	-315	315	0	283	137
Battery	315	-315	315	-315	-315	0	197	96

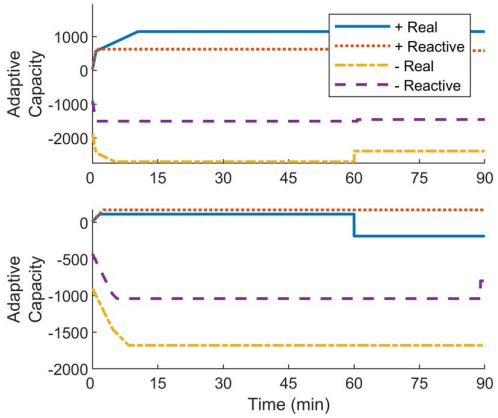

Fig. 9. Flexibility at power factor angles in the direction of real (kW) and reactive (kVAR) power. The top plot is under normal operation and the bottom is when network connection is lost.

stored energy, and therefore can maintain its output of 197 kW for one hour. The aggregation of the assets adaptive capacity is shown in Fig. 8. The temporal flexibility in real and reactive power is shown in the bottom of Fig. 9.

C. Discussion

Results of the case study bring to light a few important concepts in reliability and resilience of power systems. It can be stated that even when the network was lost the system is reliable, as no load needed to be shed. However, when evaluating the systems using the proposed adaptive capacity metric there is a quantifiable impact to the resilience of the system. This is visible by examining the difference in manifolds and easy to distinguish by inspection of Fig. 9. The top plot shows that there is adaptive capacity in the real and reactive power in all directions, but is most "constrained" by the real (1,149 kW) and reactive (627 kVAR) power in the positive direction. In the case of losing network connection this constrain becomes 113 kW and 171 kVAR. Therefore, the ability to adapt to a future disturbance has been dramatically reduced. In fact, the system will lose capability to supply the real power necessary in one hour when the battery storage runs out of energy. This will result in a loss of the ability to maintain the frequency of the system if loads are not shed.

VI. Conclusion and Future Work

In this paper, we present a resilience metric based on adaptive capacity for modern distribution systems that have a high penetration of distributed resources. The proposed metric provides insight to the ability to control aggregated assets in terms of real and reactive power over time. The metric is used to analyze a microgrid under different scenarios, such as a loss of network connection. The metric is demonstrated indicating the distributed resources can maintain the loads when the connection is lost, however, the systems adaptive capacity is greatly reduced, having very little capability to support stability of voltage and frequency if further disruptions occur.

Future work with respect to improvements to the adaptive capacity metric include replacing the linear ramp rates with non-linear rates. Similarly, the real and reactive bounds in certain assets which are not constant, should be replaced by a function or table to provide better accuracy in the metric. For example, the ramp rate of a hydro generator is not constant but dependant on the head pressure. Additionally, the maximum power is also dependant on the pressure and should be reflected in the metric.

Acknowledgment

This material is based upon work supported by the US Department of Energy's Office of Energy Efficiency and Renewable Energy (EERE) under the Solar Energy Technology Office Award Number DE-0008775. We thank our colleagues Professor Masood Parvania, Phd and Mohamad El Hariri, PhD. from the University of Utah who provided insight and expertise that assisted this research. Effort performed through Department of Energy under U.S. DOE Idaho Operations Office Contract DE-AC07-05ID14517, as part of the Resilient Control and Instrumentation Systems (ReCIS) program of Idaho National Laboratory. We would also like to thank National Science Foundation Computer and Information Science and Engineering (CISE), award number 1846493 of the Secure and Trustworthy Cyberspace (SaTC) program: Formal TOols foR SafEty aNd. Security of Industrial Control Systems (FORENSICS).

References

[1] Institute of Electrical and Electronics Engineers, "Ieee guide for electric power distribution reliability indices," *IEEE Std 1366-2012 (Revision of IEEE Std 1366-2003)*, pp. 1–43, May 2012.

[2] M. McGranaghan, M. Olearczykm, and C. Gellings, "Enhancing distribution resiliency: Opportunities for applying innovative technologies," Electric Power Research Institute, Tech. Rep. 1026889, 2013.

[3] H. L. Willis, *Power Distribution Planning Reference Book*. CRC Press, 2004.

[4] U.S. Department of Energy Office of Electricity Delivery and Energy Reliability, "Economic benefits of increasing electric grid resilience to weather outages," Executive Office of the President, Tech. Rep., 2013.

[5] L. Che, M. Khodayar, and M. Shahidehpour, "Only connect: Microgrids for distribution system restoration," *IEEE Power and Energy Magazine*, vol. 12, no. 1, pp. 70–81, Jan 2014.

[6] M. Fan, Z. Zeng, E. Zio, R. Kang, and Y. Chen, "A stochastic hybrid systems model of common-cause failures of degrading components," *Reliability Engineering & System Safety*, vol. 172, pp. 159 – 170, 2018. [Online]. Available: http://www.sciencedirect.com/science/article/pii/S0951832017304143

[7] W. Parker, B. K. Johnson, C. Rieger, and T. McJunkin, "Identifying critical resiliency of modern distribution systems with open source modeling," in *2017 Resilience Week (RWS)*, Sep. 2017, pp. 113–118.

[8] D. A. Reed, M. D. Powell, and J. M. Westerman, "Energy supply system performance for hurricane katrina," *Journal of Energy Engineering*, vol. 136, no. 4, pp. 95–102, 2010. [Online]. Available: https://ascelibrary.org/doi/abs/10.1061/%28ASCE%29EY.1943-7897.0000028

[9] D. Henry and J. E. Ramirez-Marquez, "On the impacts of power outages during hurricane sandy—a resilience-based analysis," *Systems Engineering*, vol. 19, no. 1, pp. 59–75, 2016. [Online]. Available: https://onlinelibrary.wiley.com/doi/abs/10.1002/sys.21338

[10] A. Imteaj, M. H. Amini, and J. Mohammadi, "Leveraging decentralized artificial intelligence to enhance resilience of energy networks," 2019.

[11] H. L. Willis and R. R. Schrieber, *Aging Power Delivery Infrastructures*, 2nd ed. Boca Raton, FL: CRC Press, 2013.

[12] R. Campbell, "Weather-related power outages and electric system resiliency," CRS Report for Congress, Tech. Rep., 01 2013.

[13] B. Anderson and M. Bell, "Lights out impact of the august 2003 power outage on mortality in new york, ny," *Epidemiology (Cambridge, Mass.)*, vol. 23, pp. 189–93, 03 2012.

[14] E. Hollnagel, D. Woods, and N. Leveson, *Resilience Engineering: Concepts and precepts*. Ashgate Publishing, 2006.

[15] Electric Power Research Institute, "Grid resiliency," https://www.epri.com/#/grid_resiliency, accessed: 1/30/2020.

[16] National Acedemies of Sciences, Engineering, and Medicine, "Enhancing the resilience of the nation's electricity system," https://doi.org/10.17226/24836, 2017.

[17] Sandia National Laboratories, "Energy: Grid resilience," https://energy.sandia.gov/programs/electric-grid/resilient-electric-infrastructures/, accessed: 2/6/2020.

[18] H. Mehrpouyan, B. Haley, A. Dong, I. Y. Tumer, and C. Hoyle, "Resiliency analysis for complex engineered system design," *AI EDAM*, vol. 29, no. 1, pp. 93–108, 2015.

[19] H. Mehrpouyan, D. Giannakopoulou, G. Brat, I. Y. Tumer, and C. Hoyle, "Complex engineered systems design verification based on assume-guarantee reasoning," *Systems Engineering*, vol. 19, no. 6, pp. 461–476, 2016.

[20] U.S. Department of Homeland Security, "Presidential policy directive 21 implementation: An interagency security committee white paper," 2015.

[21] C. G. Rieger, D. I. Gertman, and M. A. McQueen, "Resilient control systems: Next generation design research," in *2009 2nd Conference on Human System Interactions*, May 2009, pp. 632–636.

[22] "Energy policy act of 2005," Public Law No. 109-58, 119 Stat. 594, 2005.

[23] Congressional Research Service, "Electric reliability and power system resilience," CRS Insight, Tech. Rep., 2018, https://www.everycrsreport.com/reports/IN10895.html.

[24] K. Tierney and M. Bruneau, "Conceptualizing and measuring resilience: A key to disaster loss reduction," *TR News*, vol. 250, pp. 14–17, 05 2007.

[25] M. Panteli, D. N. Trakas, P. Mancarella, and N. D. Hatziargyriou, "Power systems resilience assessment: Hardening and smart operational enhancement strategies," *Proceedings of the IEEE*, vol. 105, no. 7, pp. 1202–1213, July 2017.

[26] S. M. Rinaldi, J. P. Peerenboom, and T. K. Kelly, "Identifying, understanding, and analyzing critical infrastructure interdependencies," *IEEE Control Systems Magazine*, vol. 21, no. 6, pp. 11–25, Dec 2001.

[27] M. Ouyang and L. Dueñas-Osorio, "Time-dependent resilience assessment and improvement of urban infrastructure systems," *Chaos (Woodbury, N.Y.)*, vol. 22, p. 033122, 09 2012.

[28] D. Henry and J. E. Ramirez-Marquez, "Generic metrics and quantitative approaches for system resilience as a function of time," *Reliability Engineering & System Safety*, vol. 99, pp. 114 – 122, 2012. [Online]. Available: http://www.sciencedirect.com/science/article/pii/S0951832011001748

[29] M. Ouyang, "A three-stage resilience analysis framework for urban infrastructure systems," *Structural Safety*, vol. 36-37, pp. 23–31, 03 2012.

[30] C. G. Rieger, "Resilient control systems practical metrics basis for defining mission impact," in *2014 7th International Symposium on Resilient Control Systems (ISRCS)*, Aug 2014, pp. 1–10.

[31] D. Woods, *Resilience Engineering: Concepts and Precepts*. CRC Press, 2017.

[32] T. R. McJunkin and C. G. Rieger, "Electricity distribution system resilient control system metrics," in *2017 Resilience Week (RWS)*, Sep. 2017, pp. 103–112.

[33] C. Chen, J. Wang, F. Qiu, and D. Zhao, "Resilient distribution system by microgrids formation after natural disasters," *IEEE Transactions on Smart Grid*, vol. 7, no. 2, pp. 958–966, March 2016.

[34] S. Chanda and A. K. Srivastava, "Defining and enabling resiliency of electric distribution systems with multiple microgrids," *IEEE Transactions on Smart Grid*, vol. 7, no. 6, pp. 2859–2868, Nov 2016.

[35] P. Dehghanian, S. Aslan, and P. Dehghanian, "Quantifying power system resiliency improvement using network reconfiguration," in *2017 IEEE 60th International Midwest Symposium on Circuits and Systems (MWSCAS)*, Aug 2017, pp. 1364–1367.

[36] S. Yao, T. Zhao, P. Wang, and H. Zhang, "Resilience-oriented distribution system reconfiguration for service restoration considering distributed generations," in *2017 IEEE Power Energy Society General Meeting*, July 2017, pp. 1–5.

[37] M. H. Oboudi, M. Mohammadi, and M. Rastegar, "Resilience-oriented intentional islanding of reconfigurable distribution power systems," *Journal of Modern Power Systems and Clean Energy*, vol. 7, no. 4, pp. 741–752, Jul 2019. [Online]. Available: https://doi.org/10.1007/s40565-019-0567-9

[38] M. Khomami, K. Jalilpoor, M. Kenari, and M. Sepasian, "Bi-level network reconfiguration model to improve the resilience of distribution systems against extreme weather events," *IET Generation Transmission & Distribution*, 05 2019.

[39] H. Wang, S. Wang, L. Yu, and P. Hu, "A novel planning-attack-reconfiguration method for enhancing resilience of distribution systems considering the whole process of resiliency," *International Transactions on Electrical Energy Systems*, vol. n/a, no. n/a, p. e12199, 2019, e12199 ITEES-19-0457.R1. [Online]. Available: https://onlinelibrary.wiley.com/doi/abs/10.1002/2050-7038.12199

[40] M. Zare, A. Abbaspour, M. Fotuhi-Firuzabad, and M. Moeini-Aghtaie, "Increasing the resilience of distribution systems against hurricane by optimal switch placement," in *2017 Conference on Electrical Power Distribution Networks Conference (EPDC)*, April 2017, pp. 7–11.

[41] M. M. Hosseini, A. Umunnakwe, and M. Parvania, "Automated switching operation for resilience enhancement of distribution systems," in *2019 IEEE Power Energy Society General Meeting (PESGM)*, 2019, pp. 1–5.

[42] M. M. Hosseini and M. Parvania, "Quantifying impacts of automation on resilience of distribution systems," *IET Smart Grid*, 02 2020.

[43] E. Ciapessoni, D. Cirio, A. Pitto, P. Marcacci, and M. Sforna, "Security-constrained redispatching to enhance power system resilience in case of wet snow events," in *2018 Power Systems Computation Conference (PSCC)*, June 2018, pp. 1–7.

[44] G. Huang, J. Wang, C. Chen, J. Qi, and C. Guo, "Integration of preventive and emergency responses for power grid resilience enhancement," *IEEE Transactions on Power Systems*, vol. 32, no. 6, pp. 4451–4463, Nov 2017.

[45] H. Khaloie, A. Abdollahi, M. Rashidinejad, and P. Siano, "Risk-based probabilistic-possibilistic self-scheduling considering high-impact low-probability events uncertainty," *International Journal of Electrical Power & Energy Systems*, vol. 110, pp. 598 – 612, 2019. [Online]. Available: http://www.sciencedirect.com/science/article/pii/S0142061518304290

[46] H. Nguyen, J. Muhs, and M. Parvania, "Assessing impacts of energy storage on resilience of distribution systems against hurricanes," *Journal of Modern Power Systems and Clean Energy*, 07 2019.

[47] M. Rezaeimozafar, M. H. Amini, and M. Moradi, "Innovative appraisement of smart grid operation considering large-scale integration of electric vehicles enabling v2g and g2v systems," *Electric Power Systems Research*, vol. 154, pp. 245–256, 01 2018.